5-2023

Separating the R vs. S Enantiomers of a Quinoline Aimed at Inhibiting the Allosteric Binding Pocket of HIV-1 Integrase

Madison Canfield
The University of Southern Mississippi

Separating the R vs. S Enantiomers of a Quinoline Aimed at Inhibiting the Allosteric Binding Pocket of HIV-1 Integrase

by

Madison Canfield

A Thesis
Submitted to the Honors College of
The University of Southern Mississippi
in Partial Fulfillment
of Honors Requirements

2023

Approved by:

Matthew Donahue, Ph.D., Thesis Advisor,
School of Mathematics and Natural Sciences

Theofanis Kitsopoulos, Ph.D., Director,
School of Mathematics and Natural Sciences

Sabine Heinhorst, Ph.D., Dean
Honors College

ABSTRACT

HIV-1 is a retroviral disease that infects CD4+ T cells in the body. Once inside the body, HIV-1 uses human cell machinery to replicate and reproduce using several enzymes to reverse transcribe viral RNA to DNA and integrate the viral DNA into the human genome to reproduce. Several drugs, such as NRTIs, INSTIs, NNRTIs, and PIs, have been created to inhibit specific parts of the viral life cycle and are used in combination to fight HIV-1. However, these medications face challenges of viral mutation and resistance, which increases the importance of creating more potent and effective drugs. Recently, a new class of drugs called ALLINIs have emerged and work by preventing HIV-1 integrase from integrating viral DNA into the host by binding to IN and blocking the IN-LEDGF/p75 binding site on the host. In previous studies, a substituted quinoline further derivatized at position 7 was created and found to be potent in carrying out this action as well as impacting viral maturation via inducing multimerization of IN. In this thesis, a further substituted quinoline structure was synthesized with a R and S enantiomer branching off position 3, where the S form is hypothesized to be more potent in inhibiting HIV-1. A separation attempt was then conducted using a chiral coupling compound. After analysis of the completed reaction by TLC and ^{1}H NMR, the molecule failed to separate into two distinct diastereomers. However, once separated the molecules can be characterized using the Mosher ester model and individually assessed on their multimerization effects on IN to see which diastereomer is more active against HIV-1 and may become a new potent drug in fighting the disease.

Keywords: HIV-1, integrase, quinoline, retrovirus, drug synthesis

DEDICATION

This Honors College thesis is dedicated to all family, friends, peers, and mentors who have helped me through my time at the University of Southern Mississippi. I want to specifically dedicate this paper to my parents and loved ones who have supported me throughout this whole process and encouraged me to finish this thesis when I felt like giving up. I want to also specifically dedicate this to the Donahue Research Group for their constant mentoring through this entire research experience and for helping me undertake a thesis outside of my major.

ACKNOWLEDGMENTS

I want to thank all the members of Donahue Research Group and the Honors College for helping with the creation of my thesis. Specifically, I would like to thank my advisor, Dr. Matthew Donahue, for mentoring me through this project and giving countless advice for this research. I would also like to thank my other mentor and lab mate, Jack Patterson, for teaching me how to conduct my experiments, use all the lab equipment, and understand the foreign language that is Organic Chemistry.

I want to thank all the advisors and professors I have had during my time in the Honors College. The colloquium, seminar, and thesis classes taught me the basis of research and prepared me to complete this thesis throughout my entire career at USM. My advisors have also provided countless encouraging words when I felt discouraged during this thesis process.

Lastly, I want to acknowledge my family and best friends for their constant support throughout this process. They have provided so much support, advice, and love throughout this endeavor and always encouraged me to not give up. I truly could have not completed this thesis without their help and motivation, and I will be forever grateful to have had them in my life.

TABLE OF CONTENTS

LIST OF TABLES

LIST OF ILLUSTRATIONS

LIST OF ABBREVIATIONS

ATLAS	Antiretroviral Therapy as Long-Acting Suppression
ARV	Antiretroviral
CA	CCR5 Antagonist
CAM	Ceric Ammonium Molybdate
cART	Combined Antiretroviral Therapy
CCD	Catalytic Core Domain
CTD	C-terminal Domain
DCM	Dichloromethane
DFT	Density Functional Theory
DKA	β-diketo acid
DMSO	Dimethyl Sulfoxide
FDA	Food and Drug Administration
FDC	Fixed-Dose Combination
FI	Fusion Inhibitor
FLAIR	First Long-Acting Injectable Regimen
ART	Antiretroviral Therapy
HPLC	High Performance Liquid Chromatography
IN	Integrase
INSTI	Integrase Strand Transfer Inhibitor
LEDGF/p75	Lens Epithelium-Derived Growth Factor
MTPA	α-methoxy-α-trifluoromethylphenylacetic acid or Mosher's Acid
NMR	Nuclear Magnetic Resonance Spectroscopy

NRTIs	Nucleoside/Nucleotide Reverse Transcriptase Inhibitors
NNRTIs	Non-Nucleoside Reverse Transcriptase Inhibitors
PAI	Post-Attachment Inhibitor
PE	Pharmacokinetic Enhancer
PI	Protease Inhibitor
PR	Protease
RNP	Ribonucleoprotein Complex
RT	Reverse Transcriptase
TBAF	Tetrabutylammonium Fluoride
TBS	Tris-buffered Saline
TBSMAC	(tert-Butyldimethylsilyloxy) malononitrile
TLC	Thin Layer Chromatography

CHAPTER I: BACKGROUND

HIV-1 Life Cycle Overview

HIV-1 is a retrovirus that infects 38 million people worldwide. The virus is spread via intercourse and exchange of bodily fluids or blood. Once infected, people experience flu like symptoms due to the attack on the cells of the immune system.[1] The virus targets CD4+ helper T cells and goes through a process of reverse transcription and integration to replicate the viral genes into the host. In its envelope, glycoprotein 120 (gp120) assists in viral attachment while glycoprotein 41(gp41) mediates viral fusion. Additionally, HIV-1 utilizes its retroviral gene *pol* to code for reverse transcriptase (RT), protease (PR), and integrase (IN), which aid in transcribing its viral RNA into host DNA.[2]

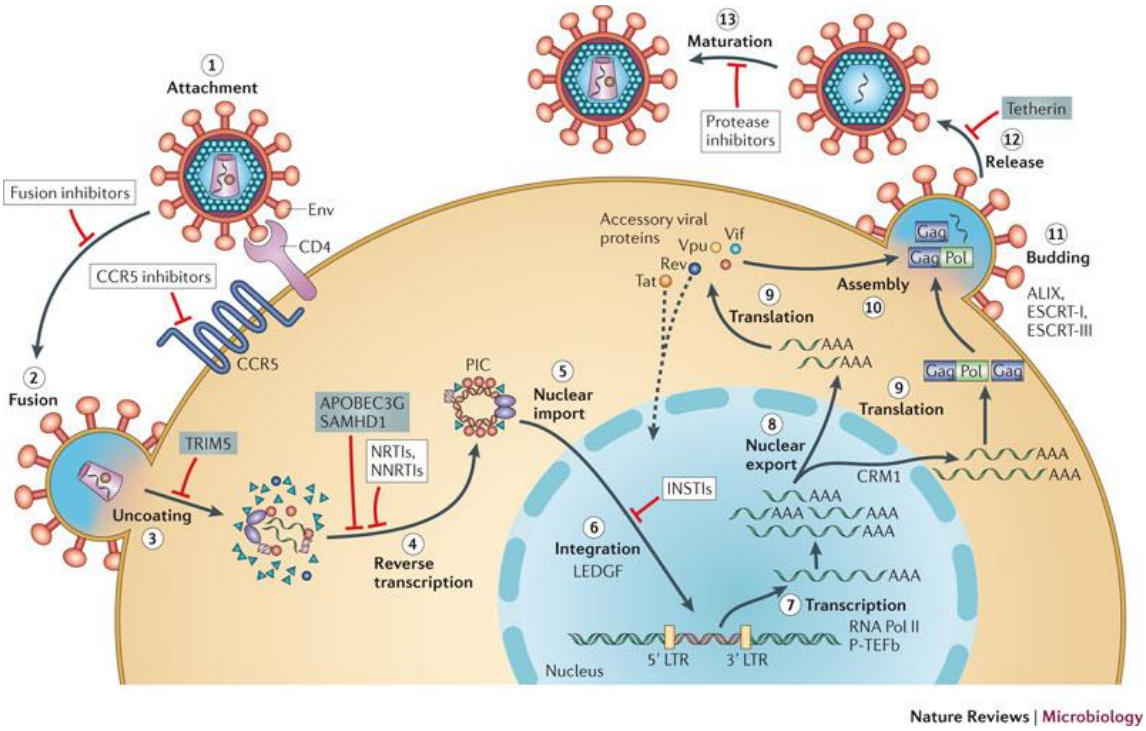

Figure 1. Life Cycle of HIV-1 with the Location of Inhibitor Interference. Adapted from[2]

As seen in Figure 1, HIV-1 begins its replication cycle by attaching to receptors on host CD4+ T cells and enters the cell by inducing conformational changes via interactions with gp120 and the CD4 cell receptors. The virus then fuses with the cell membrane and enters the host cell, and the genetic information is uncoated within the host. Single-stranded viral RNA is then reverse transcribed into double-stranded DNA with the assistance of the viral enzyme RT and forms the pre-integration complex, PIC. HIV-1 then integrates its genes into the host cell using the integrase enzyme to allow the viral gene products to be spread to new cells upon host replication. Transcription, translation, and assembly of viral products can then be conducted, and the immature virus can bud of the host cell. Maturation of the virus then occurs with the help of GAG proteins and the protease enzyme.[2]

Antiretroviral Drug Therapies and Current Treatment Regime

Over 30 different types of ARV drugs exist under eight classes targeting different parts of HIV-1's life cycle. The first class of drugs to be approved by the FDA are the nucleoside/nucleotide reverse transcriptase inhibitors (NRTIs), which depend on phosphorylation to prevent the formation of viral phosphodiester bonds in the reverse transcription process. Examples of approved drugs of NRTIs include abacavir and tenofovir. Additionally, non-nucleoside reverse transcriptase inhibitors (NNRTIs) target RT by creating a hydrophobic pocket in the active site to reduce polymerase activity including drugs such as efavirenz. Protease inhibitors (PIs) target protease and the viral maturation process such as atazanavir. The most recent class of FDA approved drugs are the integrase strand transfer inhibitors (INSTIs) target integrase in the integration of viral DNA, including raltegravir, elvitegravir, and

dolutegravir. Fusion inhibitors, CCR5 receptor antagonists, gp120 and gp41 entry inhibitors, and CD4 T lymphocyte post-attachment inhibitors are the remaining types of drugs that are specific targets of HIV-1. Ritonavir and cobiscistat are also used to boost the pharmacokinetic profiles of PIs and elvitegravir.[3] The points at which these inhibitors act in the HIV-1 life cycle can be visually seen in Figure 1.

Table 1. Timeline of FDA Approved HIV-1 Drugs by Year and Classification.[4]

	1987-1994	*1995-1999*	*2000-2004*	*2005-2011*	*2012-2016*	*2017-2021*
NRTI	Zidovudine Didanosine Zalcitabine Stavudine	Lamivudine Abacavir	Didanosine EC Emtricitabine Tenofovir DF			
NNRTI		Nevirapine Delavirdine Efavirenz		Etravirine Nevirapine XR Rilpivirine		Doravirine
PI		Saquinavir Indinavir Ritonavir Nelfinavir Amprenavir	Fosamprenavir Atazanavir	Tipranavir Darunavir		
FDC		Combivir	Kaletra Trizivir Epzicom Truvada	Atripla Complera	Stribild Triumeq Evotaz Genvoya Prezcobix Descovy Odefsey	Juluca Biktarvy Cimduo Symfi Symfi Lo Symtuza Delstrigo Temixys Dovato Cabenuva
FI			Enfuvirtide			
INSTI				Raltegravir	Dolutegravir Elvitegravir	Cabotegravir
PE					Cobicistat	
CA				Maraviroc		
AI						Fostemsavir
PAI						Ibalizumab-uiyk

Current HIV-1 treatment involves a combination of antiretroviral (ARV) drugs called combined antiretroviral therapy (cART) therapy to help manage the replication and spread of the virus and reduce the chance of contracting opportunistic

infections due to the suppressed immune system. The three-drug regime for an infected person consists of two NRTIs and a drug from either the INSTI, NNRTI, or boosted PI categories, also known as a fixed dose combination, FDC.[4] Continuous research on treatment methods and drug development for HIV-1 is conducted as the virus readily mutates to overcome the effectiveness of drugs. All FDA approved drugs can be seen in **Table 1** above with the drug class listed in the left-hand column and the years listed on the top row. For this keystone research, the focus is on drug development for inhibiting HIV-1 integrase at its allosteric pocket.

CHAPTER II: INTRODUCTION

Structure and Role of HIV-1 Integrase

HIV-1 IN is composed of 288 amino acids and contains three domains: an N-terminal domain (NTD), catalytic core domain (CCD), and C-terminal domain (CTD). The NTD domain contains the C40 and C43 cysteine residues and the H12 and H16 histidine residues, which forms the zinc-dependent motif required for IN multimerization. The CCD contains three conserved negatively charged aspartic acid and glutamic acid residues, D64, D116, and E152, or the DDE motif, which bind metal ions, Mg^{2+} and Mn^{2+} that assist in the catalytic function of integration. The CTD domain is the least conserved domain and non-specifically binds DNA[5]. These functional domains form a tetramer for viral DNA and host DNA to bind to IN. The structure of IN can be seen in **Figure 6**. Additionally, integration of viral genes depends on the interaction of the IN-binding domain (IBD) and LEDGF/p75 growth factor. LEDGF/p75 attaches IN to the host chromatin through its N-terminal segment and binds to IN through its C-terminal at the IN CCD interface.[6]

Within the HIV-1 life cycle, HIV-1 IN assists in 3' processing and DNA strand transfer. During 3' processing, IN helps to form the stable synaptic complex (SSC) by binding the U3 and U5 ends together of viral DNA. Then, IN processes the 3' ends of viral DNA to create the CA_{OH}-3' hydroxyl groups that act as substrates for DNA strand transfer. Once entering the host nucleus and finding and host acceptor site, strand transfer can begin with the 3' hydroxyl ends on the viral DNA attacking the phosphodiester bonds of the host DNA while the viral 3' ends remain in close

contact. The viral DNA 3' hydroxyl ends can then be attached to the 5' phosphate ends on the target host DNA to form the integrated provirus that can now produce more viruses.[7,8]

Active Site IN Inhibitors

INSTIs are active site IN inhibitors function to prevent the strand transfer between IN and the host chromosomal DNA by binding to the enzymatic active site. Some INSTIs also can also inhibit the 3' end processing as well. INSTIs have a small window of successful inhibition as integration of a provirus only requires two integration events out of 50-100 transferred copies of IN must occur. INSTIs must act at the point after reverse transcription about 4-16 hours post infection and lead to the build-up of 2-long terminal repeat circles of viral DNA and cause mutations in the IN gene. INSTIs work by binding to the active site of IN after the viral DNA changes the conformation of IN and binds to the metal ions of the DDE motif of the CCD. The structure of these INSTIs compounds involves a metal-binding, or catalytic, portion and an enzyme-binding formation. The enzyme-binding portion contains hydrophobic aromatic groups that allow the compound to bind to the hydrophobic pocket created by the binding of viral DNA to IN. The metal-binding portion represses the metal ions at the IN active site that are required for proper enzymatic activity.[5]

Raltegravir became the first FDA approved INSTI drug in 2007, created by MERCK. The molecular structure of raltegravir includes a β-diketo acid (DKA) motif that combines with the metal ions in the IN active site to inhibit strand transfer, where the drug had a more potent effect when acting after the 3' ends have been processed.

Among many surveyed potential drugs, MK-0518, or raltegravir, was selected as the safest and most potent drug that selected for strand transfer inhibition and worked with other inhibitor drugs in combination.[9] In clinical trials, raltegravir was administered as a twice daily treatment and helped increase the CD4+ T-cell counts while reducing the number of viral copies after 48 weeks in subjects who had previously been resistant to ARV drugs with fewer instances of adverse effects compared to another INSTI drug, efavirenz.[10] Unfortunately, HIV-1 mutations quickly arose, creating resistance to raltegravir and having a 25% fail rate within the first two days of treatment.[9]

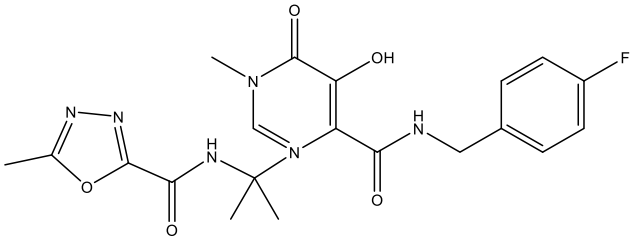

Figure 2. Molecular Structure of Raltegravir.

Elvitegravir became the second FDA approved drug in 2012 and has a monoketo motif that serves as an alternative to the DKA motif.[9] It is administered with a combination of drugs put into one pill, called Stribild and requires boosting and food intake upon taking the pill. In clinical trials, the drug proved 88% effective in viral suppression than efavirenz at 84% efficiency with

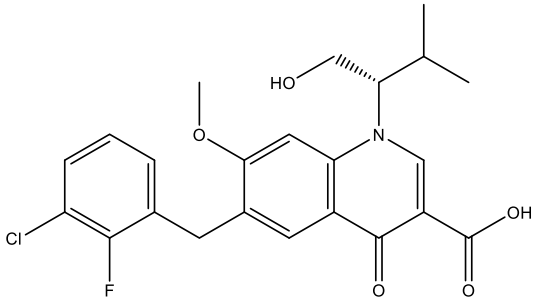

Figure 3. Molecular Structure of Elvitegravir.

significantly less psychological effects[11]. However, like raltegravir, HIV-1 showed resistance to elvitegravir.

Dolutegravir became FDA approved in 2013 and showed a higher resistance to mutation than elvitegravir and raltegravir. Dolutegravir in combination with complementary inhibitors, took less time to enable viral suppression with 88% of patients reaching less than 50 copies/milliliter compared to only 81% of patients taking a combination regime with efavirenz. The CD4+ T cell count was also higher for dolutegravir with 267/mm^3 compared to 208/mm^3. [12] Dolutegravir also had a higher rate of viral suppression in patients at 71% than raltegravir at 64% when used with in a cART drug regime.[13]

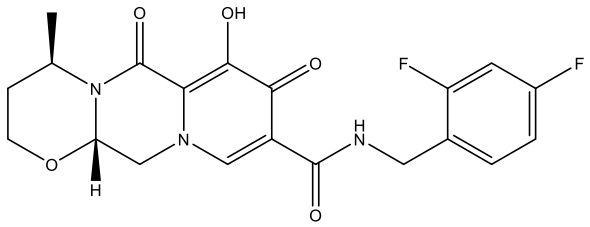

Figure 4. Molecular Structure of Dolutegravir.

Most recently, in 2019, cabotegravir became an FDA approved INSTI. It is an integrase strand transfer inhibitor that attaches to the integrase active site and prevents it from integrating the viral DNA into the host cell. Today, it is used as a combination drug called Cabenuva with both cabotegravir and rilpivirine, a non-nucleoside reverse transcriptase inhibitor. Cabenuva is given as an injection once every two months that was seen to be preferred by almost 90% of patients going through clinical trials. The clinical trials under the name Antiretroviral Therapy as Long-Acting Suppression (ATLAS) and First Long-Acting Injectable Regimen (FLAIR) showed that the drug was just as effective as using once daily pills.[14]

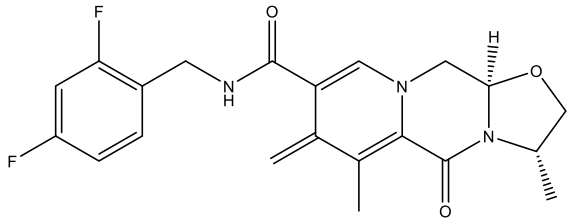

Figure 5. Molecular Structure of Cabotegravir.

Allosteric IN Inhibitors

Allosteric IN inhibitors (ALLINIs) are quinoline based compounds that interrupt the viral integration and maturation of HIV-1 by inducing IN multimerization. ALLINI compounds are made of an aromatic core, such as a quinoline or pyrimidine, which have different potencies and barriers to drug resistance of HIV-1. Compared to the active site IN inhibitors, ALLINIs are more potent during maturation and multimerize IN to prevent the interaction between IN and viral RNA to stop the ribonucleoprotein complexes, RNPs, from reaching the viral core and preventing the formation of mature HIV-1 viruses. Additionally, ALLINIs prevent IN binding to the lens epithelium-derived growth factor, LEDGF/p75, which together form the pre-integration complex.[15]

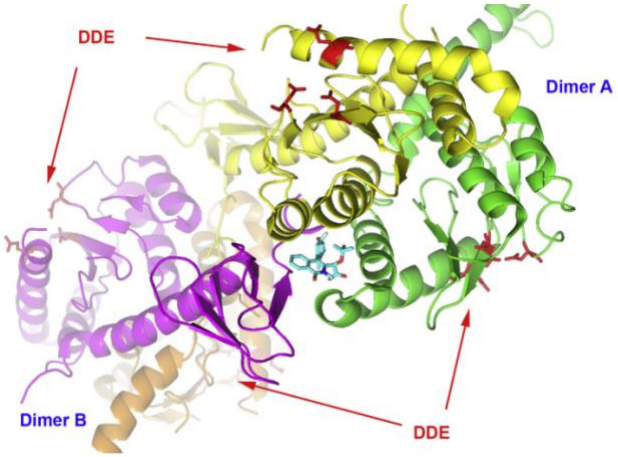

Figure 6. Example Binding of ALLINI to HIV-1 IN. The ALLINI in light blue can be seen binding to the CCD, indicated in yellow and green. Additionally, it is seen to interact with the C-terminal domain in purple on dimer B. DDE represents the catalytic triad. Adapted from[6]

The interactions that can occur between an ALLINI compound in blue and the IN tetramer can be seen in **Figure 6.** ALLINIs typically bind at the IN CCD interface away from the active site. However, ALLINIs are also able to interact with the CTD domain, which increase their antiviral potential.

The study before this keystone research was involved increasing the interaction of the compound NGJ9002 seen in **Figure 7** with the CTD domain to further increase its antiviral properties. The compound was substituted at position 7 in hopes of increasing interaction with the Y226 and W235 residues on the third subunit of HIV-1 IN. Within IN, the three domains NTD, CCD, and CTD have multiple residues as seen in **Figure 6** that have the potential to interact with different sidechains of NGJ9002 and other ALLINI compounds.

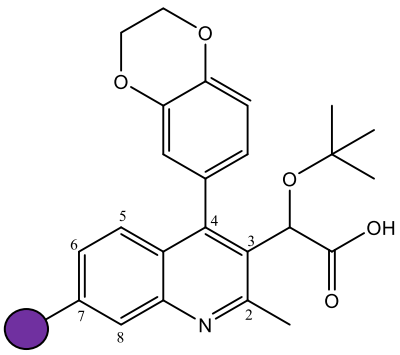

Figure 7. Molecular Structure of Compound NGJ9002.

Additional substitutions, like the 3-α-tert-butoxy acetic acid side chain on position 3, participate in hydrogen bonding with the residues H171 and T174, which imitates LEDGF/p75 binding characteristics. The 1,4-benzo dioxane group on position 4 was also present on the molecule as it maximizes interactions with the hydrophobic binding pocket of IN. These positions were kept throughout the substitution of the 7th position as they were seen to increase the compound's potency.[6]

As mentioned previously, ALLINIs are seen to impact the maturation of HIV-1 in the late stages of the life cycle via IN multimerization. While LEDGF/p75 competes with ALLINIs to bind with IN during the integration stage, the competition with LEDGF/p75 is reduced during the later stages of the replication to permit ALLINIs to multimerize IN.

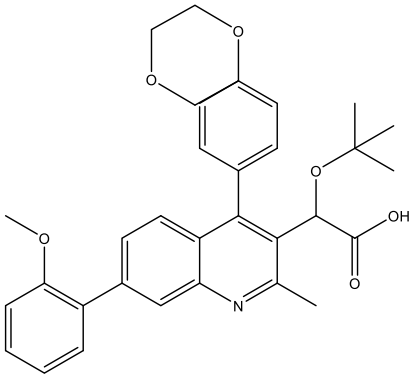

Figure 8. Molecular structure of potent substituted quinoline.

Particularly in this paper, derivations of position 7 allowed for the ALLINI to become more potent during the viral maturation stage. The results found that an ortho-substituted methoxy-benzyl group substitution at the 7th position, indicated by the purple circle in **Figure 7**, heavily increased the ALLINIs ability to interact with the third subunit of the CTD domain and multimerize IN, which prevents them from binding to viral RNA. This in turn mislocates the RNPs so they cannot reach the viral core, supporting the role that the ALLINIs can cause multimerization of IN. This molecule is represented in the **Figure 8**.[6]

In this keystone research study, the focus is on the production of drugs with addition of substituents to increase the potency of the ALLINI drugs in preventing LEDGF/p75 binding of IN of HIV-1. LEDGF/p75 binds to the CCD-CCD dimer interface away from IN's active site. These drugs play a role in blocking LEDGF/p75 in attaching to IN and create IN multimers that prevent the assembly of the pre-integration complex as seen in the previous study mentioned.

Specifically, resolving the racemic mixture of R vs S of quinoline substituted at the third position once getting to benzylic alcohol stage will allow us to see whether the R or S diastereomers is more potent in fighting against HIV-1. The racemic mixture will be attempted to be separated using chromatography and a chiral coupling agent. ^{13}C NMR analysis of each diastereomer compared to the Mosher model will help to establish absolute stereochemistry. The following methods conducted for this study have been developed and created by the Donahue Research Group.

CHAPTER III: METHODS

Preparation of the Isatoic Anhydride

12 g of 2-amino-4-methoxybenzoic acid was added to a 1000 mL single-neck round bottom flask with a stir bar and placed on the stir plate. 26 g of bis (trichloromethyl) carbonate was then added and stirred for around 5 minutes until color change from tan to dark brown. The flask was equipped with a reflux condenser, and the reaction was heated to 70 degrees Celsius and stirred around 700 rpm overnight. Following the 24-hour period, the reaction was cooled to room temperature and poured into a 4.0 L beaker containing around 750 mL of distilled water and stirred overnight. Following the 24 hr period, the heterogenous mixture was vacuum filtrated using a Buchner funnel and filter paper that was moistened with distilled water and dried overnight. ^{1}H-NMR was taken with DMSO as a solvent after compound was dry to check for compound formation.

Preparation of the Quinoline

16 g of 7-methoxy-2H-benzo[d][1,3] oxazine-2,4(1H)-dione (Compound 1 as noted in the results section) and 270 mL of DMF were added into a 500 mL single-neck round bottom flask with a stir bar and placed on the stir plate. 21 mL of ethyl 3-oxobutanoate and 3.5 grams of sodium hydroxide were then added. After 3 minutes of stirring, a reflux condenser was added to the flask and heated to around 100 degrees Celsius and stirred around 900 rpm overnight. After the 24-hour period the reaction was cooled to room temperature and poured into a 2000 mL beaker containing around 1000 mL of compacted ice and 400 mL of water and was stirred

vigorously on the stir plate for around 24 hours. After the stirring period ended, the resulting mixture was vacuum filtrated using a Buchner funnel and filter paper that was moistened with distilled water and dried overnight. ^{13}C-NMR was taken. ^{1}H-NMR was taken with DMSO as a solvent after compound was dry.

Chlorination of Quinoline

11.03 g of ethyl 4-hydroxy-7-methoxy-2-methylquinoline-3-carboxylate (2) was added to a 250 mL round bottom flask with a stir bar and clamped over a stir plate. In small portions, $POCl_3$ was added to the suspended flask. An ice bath was placed under the flask after about 15 minutes of self-heating and stirred overnight. After stirring, the mixture was poured into a 3 L beaker containing about 1000 mL of compacted ice and stirred to ensure the reaction was completely incorporated with the ice. Solid sodium hydroxide was added to the reaction until the pH read around 7.0. This took about 8 additions of around 3 grams of sodium hydroxide. The solid was vacuum filtrated out using the Buchner funnel and filter paper moistened with distilled water and dried. ^{1}H-NMR and ^{13}C-NMR were taken.

Reduction of Ethyl Ester on Quinoline to a Benzyl Alcohol

1.5 g of ethyl 4-chloro-7-methoxy-2-methylquinoline-3-carboxylate (3) and 20 mL of dichloromethane were added to a 100 mL single neck round bottom flask with a stir bar, capped, and chilled in an ice bath for 10 minutes. 17 mmol of lithium triethylborohydride was then added using a Hamilton gas tight syringe. Before addition, an argon balloon was inserted into the super hydride container to create a positive pressure, which is following by insertion of the syringe needle to pull out the

syringe's full volume (10 mmol) of argon, allowing for purging of the needle. This was repeated three times before the 10 mmol plus additionally 7 mmol was syringed out to insert into the round bottom flask. The reaction was left to stir overnight in the ice bath. To work up the reaction, the flask was removed from the ice bath, and 5 mL of acetone and 20 mL of saturated aqueous sodium chloride and stirred for 3 minutes. The mixture was then put into a 250 mL separatory funnel and the organic and aqueous phases were separated into two different Erlenmeyer flasks. The lower aqueous layer was extracted twice using 15 mL of ethyl acetate. The organic layer was washed with around 60 mL of saturated sodium chloride and was dried using magnesium sulfate then vacuum filtered. The remaining liquid organic layer was dried using the rotavap and left open overnight to rid it of any excess solvent. To further purify the compound, the product was washed with 20 ml of diethyl ether vacuum filtered and left to dry overnight. ^{1}H-NMR and ^{13}C-NMR were taken. To create a higher yield, the reaction was repeated with 0.8 g of ethyl 4-chloro-7-methoxy-2-methylquinoline-3-carboxylate (4), 10 mL of dichloromethane, and 9 mmol of lithium triethylborohydride.

Primary Alcohol Oxidation to Aldehyde

311.7 g of 4-chloro-7-methoxy-2-methylquinoline-3-yl methanol (5) and 4.371 mL of DCM were added to a 100 mL recovery flask with a stir bar. 667.5 mg of Dess-Martin periodinane was then added to the flask, and the solution turned a deep orange color. The reaction was left to stir for 4 hours. After stirring, 20 mL of ethyl acetate was added, and a large amount of white precipitate formed. The

compound was then vacuum filtrated using a Hirsch funnel with a celite plug, and the resulting solution was a clear, orange color. 10 mL of saturated aqueous sodium bicarbonate was added and stirred overnight. The material was then put into a separatory funnel and was extracted with 10 mL of ethyl acetate and washed with 50 mL of distilled water (in the aqueous layer). The organic layer was then dried with magnesium sulfate and vacuum filtered with a Hirsch funnel and Whatman paper dampened with ethyl acetate. Following the first filtration, some magnesium sulfate appeared in the resulting solution, so the solution was vacuum filtered a second time to reduce the amount of magnesium sulfate in the target solution. The resulting solution was dried using the rotavap. ^{1}H-NMR and ^{13}C-NMR were taken.

TBSMAC Reagent Addition to Create a Side Chain at C3 on the Aldehyde

228 mg of 4-chloro-7-methoxy-2-methylquinoline-3-carbaldehyde (6), 210 mg of 2-tert-butyldimethylsilyl)oxy)malononitrile, 15 mL of diethyl ether, and 170 microliters of ethanol were added to a 100 mL round bottom flask with a stir bar. The reaction was left to stir from 3/4/22 to 3/7/22. 35 mg of 4-dimethylaminopyridine was then added, and the reaction was left to stir for 24 hours. TLC analysis of the reaction's starting material and product were conducted using a 1:1 mixture of hexanes to ethyl acetate. ^{1}H-NMR and ^{13}C-NMR were taken.

Hydroxylation of the TBS Protecting Group on Ethyl Ester Side Chain

A 100 mL round bottom flask containing 0.411 g ethyl-2-((tert-butyldimethylsilyl)oxy)-2-(4-chloro-7-methoxy-2-methylquinolin-3-yl)acetate (7) and 5 mL of THF were stirred for a couple minutes. 1.94 mL of TBAF was then added to

the reaction and stirred for five minutes. A TLC was then used to monitor the reaction's progress using a 2:1 mixture of hexanes to ethyl acetate. 30 mL of sodium bicarbonate and 20 mL of ethyl acetate was added to the reaction and stirred over the weekend. The reaction was then extracted three times with 10 mL of ethyl acetate. The bottom organic layer was then washed with 50 mL of brine. The layer was then dried with magnesium sulfate and vacuum filtered. The product was left to dry under house air overnight. The product was then purified in a 50 mL column with 2:1 ethyl acetate to hexanes. 5 mL fractions were taken in test tubes using 15 mL of solvent and then analyzed by TLC. ^{1}H-NMR and ^{13}C-NMR of the column containing the desired product.

Chiral Coupling of the Quinoline at the CH position

Following the hydroxylation, 29.2 mg of ethyl 2-(4-chloro-7-methyoxy-2-methylquinolin-3-yl)-2-hydroxyacetate (8) was combined with 5 mL of DCM into a round bottom flask and stirred around 5 minutes until dissolved. 13.8 mg of DMAP and 25 mL of (1R,2S,5R)-2-isopropyl-5-methylcyclohexyl carbonochoridate were then added to the flask. The reaction was then stirred at room temperature for 5 minutes and then TLC was used using 9:1 DCM to methanol as the solvent. The reaction was then stirred over the weekend and analyzed by TLC again. The compound was dried, and an ^{1}H-NMR and ^{13}C-NMR compound were taken.

CHAPTER IV: RESULTS

Preparation of Isatoic Anhydride

The reaction yielded 15.5 g of the target compound, 7-methoxy-2H-benzo[d][1,3]oxazine-2,4(1H)-dione (1). The percent yield was 110%. **Figure 10** and **Figure 11** below show the ^{1}H NMR and ^{13}C NMR of the compound.

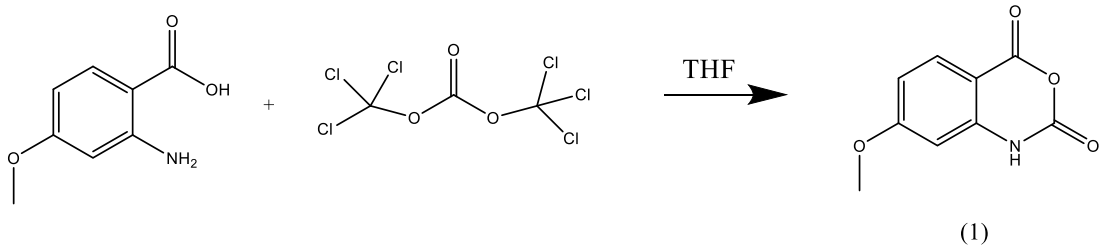

(1)

Figure 9. Scheme of Isatoic Anhydride Reaction.

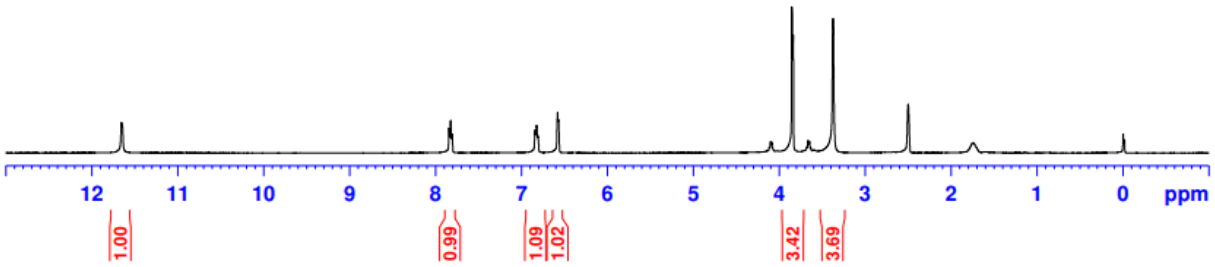

Figure 10. ^{1}H NMR of Isatoic Anhydride. ^{1}H NMR (DMSO- d6, 400 MHz) δ 3.856 (d, J= 6 Hz, 3H, OCH3), 6.58 (d, J=4.3 Hz, 1H, arCH), 6.83 (t, J = 13.6 Hz, 1H, arCH), 7.83 (t, J = 8.3 Hz, 1H, arCH), 11.65 (s, 1H, NH).

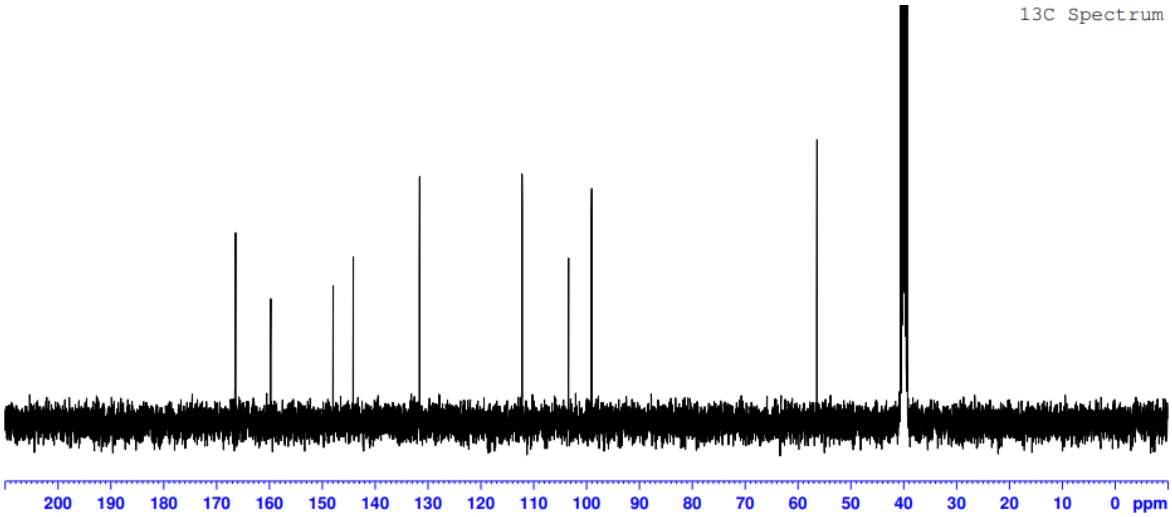

Figure 11. ^{13}C NMR of Isatoic Anhydride. ^{13}C NMR (DMSO, 400 MHz) δ 39.972 (m), 56.408 (s), 98.985 (s), 103.350 (s), 112.119 (s), 131.525 (s), 144.076 (s), 147.882 (s), 159.689 (s), 166.333 (s).

Preparation of Quinoline

The reaction yielded 11.03 g of the target compound, ethyl 4-hydroxy-7-methoxy-2-methylquinoline-3-carboxylate (2). The percent yield was 53%. **Figure 13** and **Figure 14** below show the ^{1}H NMR and ^{13}C NMR of the compound.

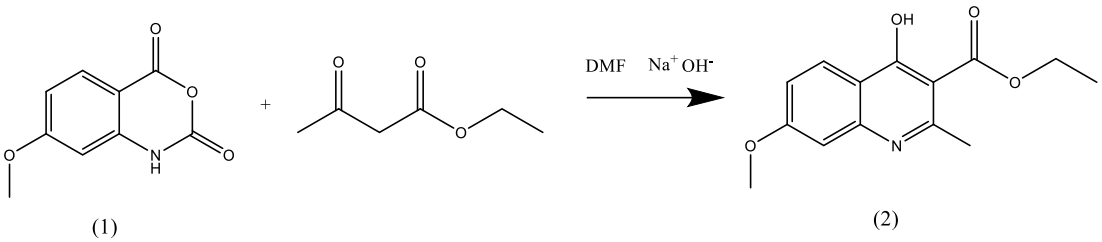

Figure 12. Scheme of Quinoline Reaction.

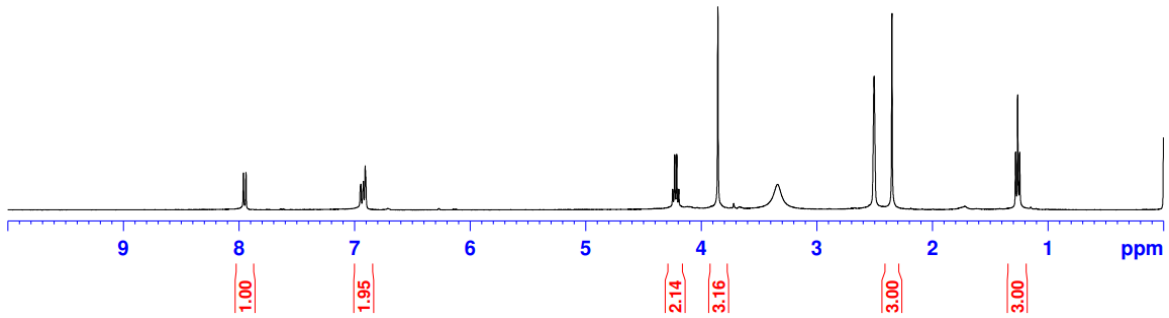

Figure 13. [1]H NMR of Quinoline. [1]H NMR (DMSO- d6, 400 MHz) δ 1.275 (t, J= 7.01 Hz, 3H, OCH2CH3), 2.379 (s, 3H, CH3), 3.890 (s, 3H, OCH3), 4.234 (q, J= 6.82 Hz, 2H, OCH2), 6.9276 (d, J = 1.81 Hz, 1H, arCH), 6.9500 (d, 1.95 Hz, 1H, arCH), 7.958 (d, J = 8.98 Hz, 1H, arCH).

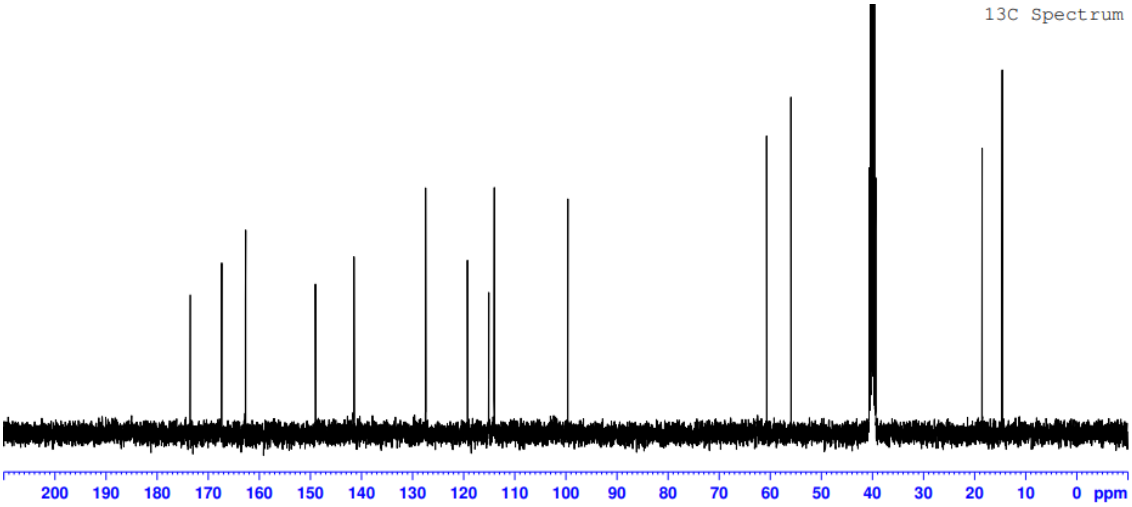

Figure 14. [13] C NMR of Quinoline. [13]C NMR (DMSO, 400 MHz) *δ* 14.595 (s), 18.523 (s), 39.969 (m), 55.925 (s), 60.686 (s), 99.538 (s), 113.922 (s), 115.016 (s), 119.186 (s), 127.357 (s), 141.386 (s), 148.926 (s), 162.616 (s), 167.288 (s), 173.433 (s).

Chlorination of Quinoline

The reaction yielded 13.25 grams of the target compound, ethyl 4-chloro-7-methoxy-2-methylquinoline-3-carboxylate (3). The percent yield was 112.2% here.

Figure 16 and **Figure 17** below show the [1]H NMR and [13]C NMR of the compound.

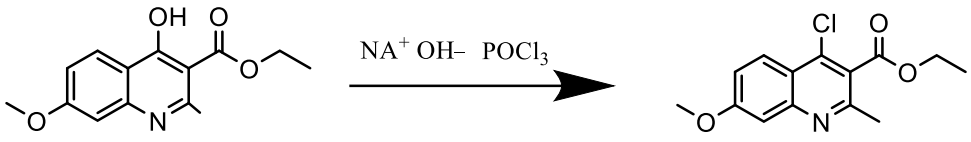

(2) (3)

Figure 15. Scheme of Quinoline Chlorination Reaction.

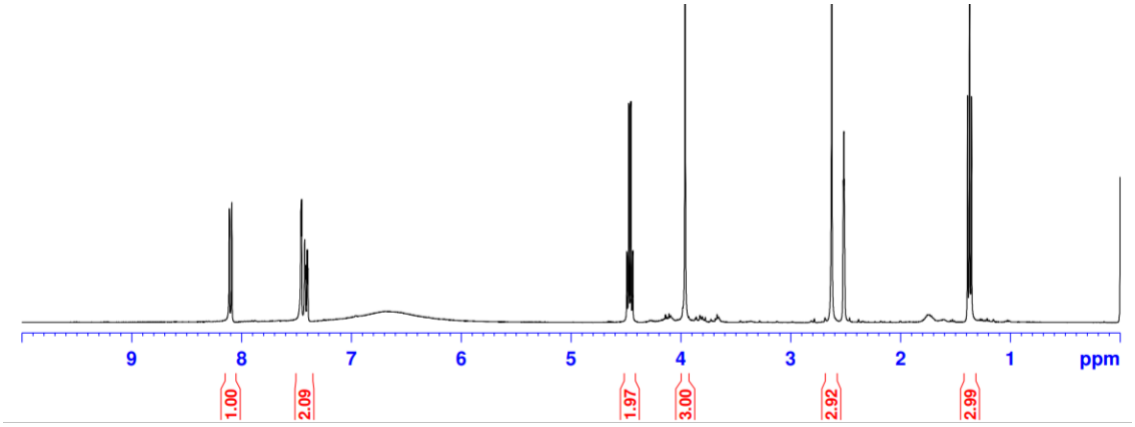

Figure 16. [1]H NMR of Chlorination of Quinoline. [1]H NMR (DMSO- d6, 400 MHz) 1.375 (t, J= 7.25, 3H, OCH2CH3), 2.521 (t, 3H, OCH3), 3.981 (s, 3H, CH3), 4.491 (q, J= 6.96 Hz, 2H, OCH2), 7.424 (d, J= 2.32 Hz, 1H, arCH), 7.4594 (d, J= 2.32 Hz, 1H, arCH), 8.111 (d, J= 9.0 Hz, 1H, arCH).

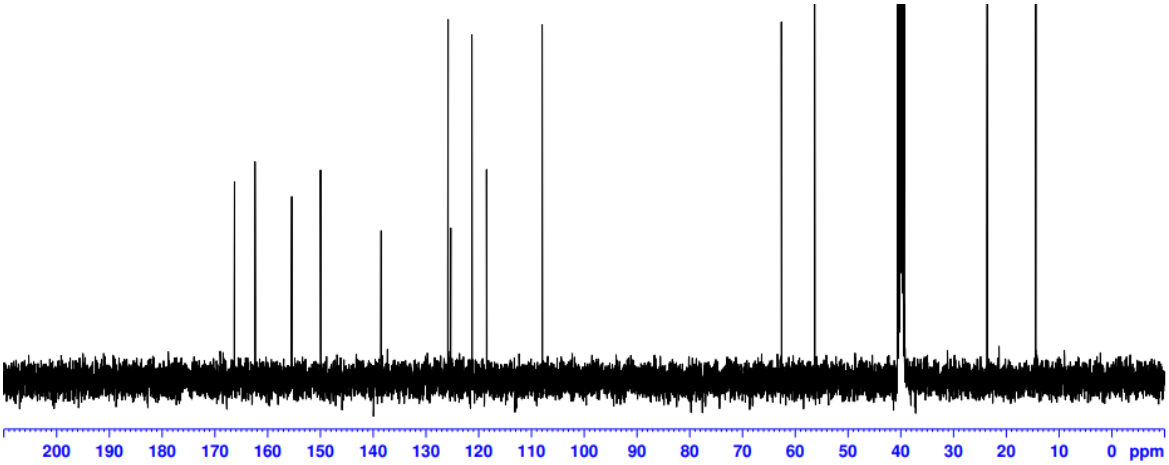

Figure 17. [13]C NMR of Chlorination of Quinoline. [13]C NMR (DMSO, 400 MHz) δ 14.392 (s), 23.612 (s), 39.948 (m), 56.296 (s), 62.591 (s), 107.885 (s), 118.412 (s), 121.199 (s), 125.233 (s), 125. 745 (s), 138.420 (s), 149.885 (s), 155.357 (s), 162.305 (s), 166.285 (s).

Reduction of Ethyl Ester on Quinoline to Benzyl Alcohol

The reaction yielded 343.8 mg of (4-chloro-7-methoxy-2-methylquinolin-3-yl) methanol (4) with 26.7% yield. **Figure 19** and **Figure 20** below show the ^{1}H NMR and ^{13}C NMR of the compound.

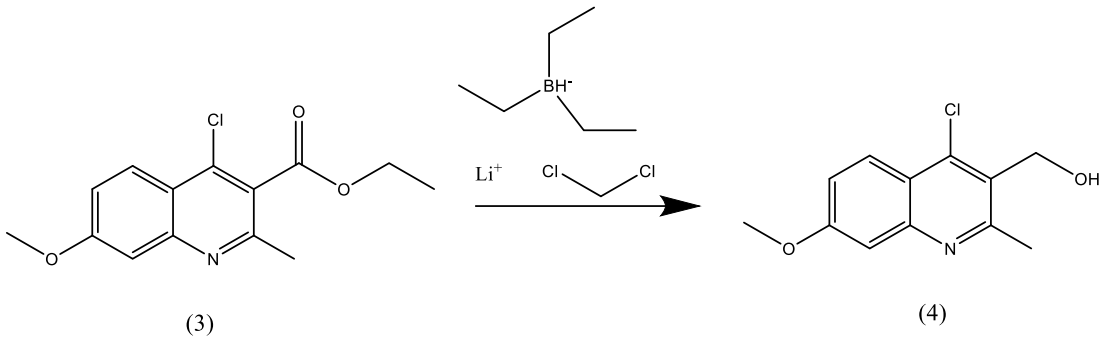

(3) (4)

Figure 18. Scheme of Reduction Reaction.

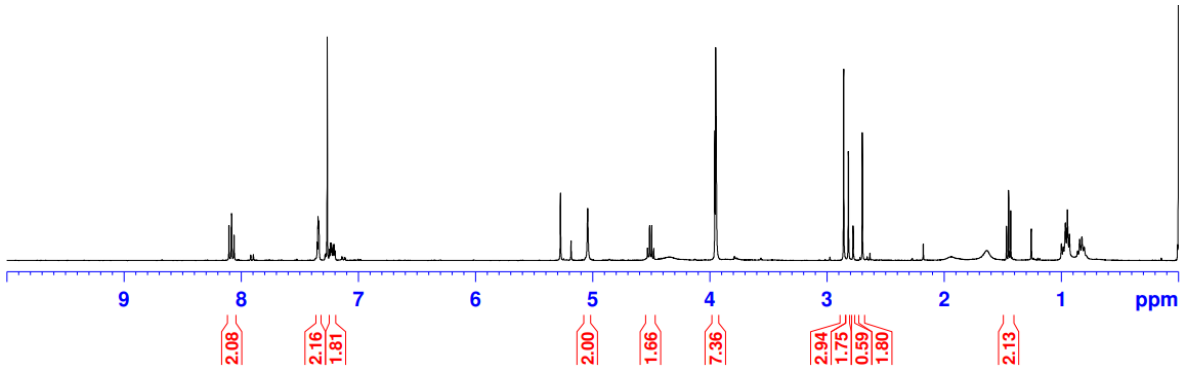

Figure 19. ^{1}H NMR of Reduction of Ethyl Ester Side Chain on Quinoline. ^{1}H NMR (CDCl3, 400 MHz) δ 5.043 (s, 2H, CH2OH), 2.857 (s, 3H, OCH3), 7.211 (d, J= 2.67 Hz, 1H, arCH), 7.234 (d, J= 2.91 Hz, 1 H, arCH).

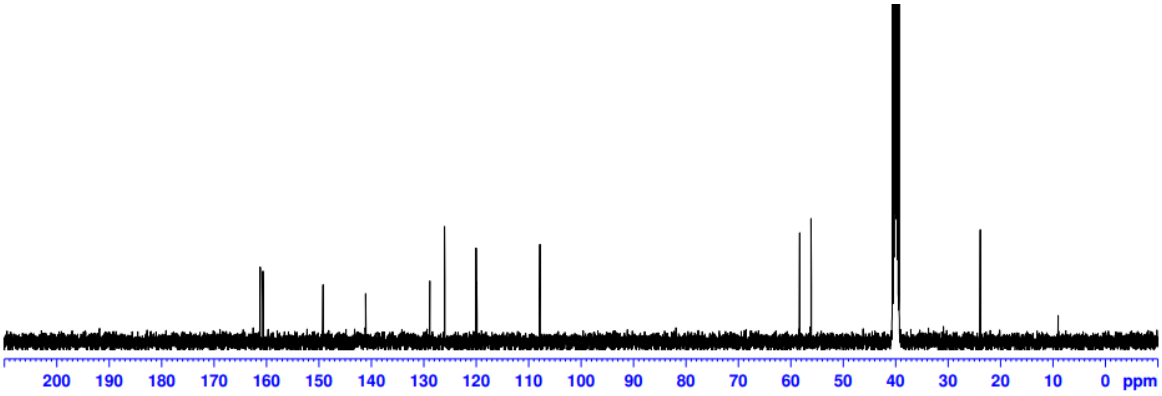

Figure 20. ^{13}C NMR of Reduction of Ethyl Ester. ^{13}C NMR (DMSO, 400 MHz) δ 9.005 (s), 23.845 (s), 39.949 (m), 56.100 (s), 58.303 (s), 107.788 (s), 119.945 (d), 125.951 (s), 128.799 (s), 140.966 (s), 149.152 (s), 149.152 (s), 160.588 (s), 161.158 (s).

Primary Alcohol Oxidation to Aldehyde

The reaction yielded 228.1 mg of the target compound, 4-chloro-7-methoxy-2-methylquinoline-3-carbaldehyde (5). The resulting yellow/orange compound had a mass of 228.1 mg. The percent yield was 75%.

Figure 22 and **Figure 23** below shows the 1H-NMR and 13C-NMR of the compound.

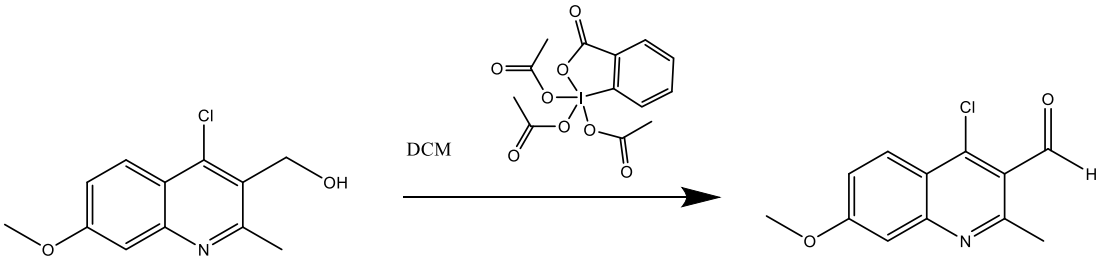

(4) (5)

Figure 21. Scheme of Alcohol Oxidation to Aldehyde Reaction.

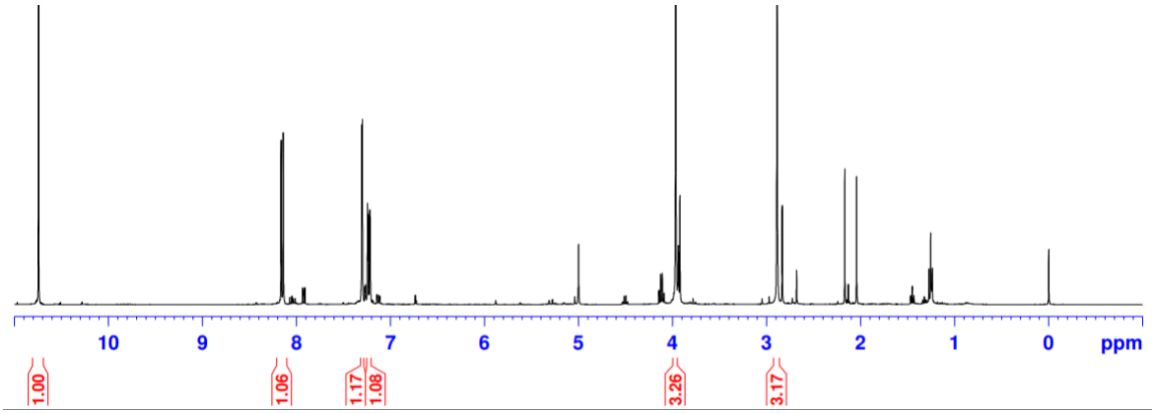

Figure 22. [1]H NMR of Aldehyde. [1]H NMR (CDCl3, 400 MHz) δ 2.891 (s, 3H, CH3), 3.967 (s, 3H, OCH3), 7.237 (dd, J = 2.4, 9.2 Hz, 1H, arCH), 7.30 (d, J = 2.4 Hz, 1H, arCH), 8.150 (d, J = 9.6 Hz, 1H, arCH), 10.742 (s, 1H, CHO).

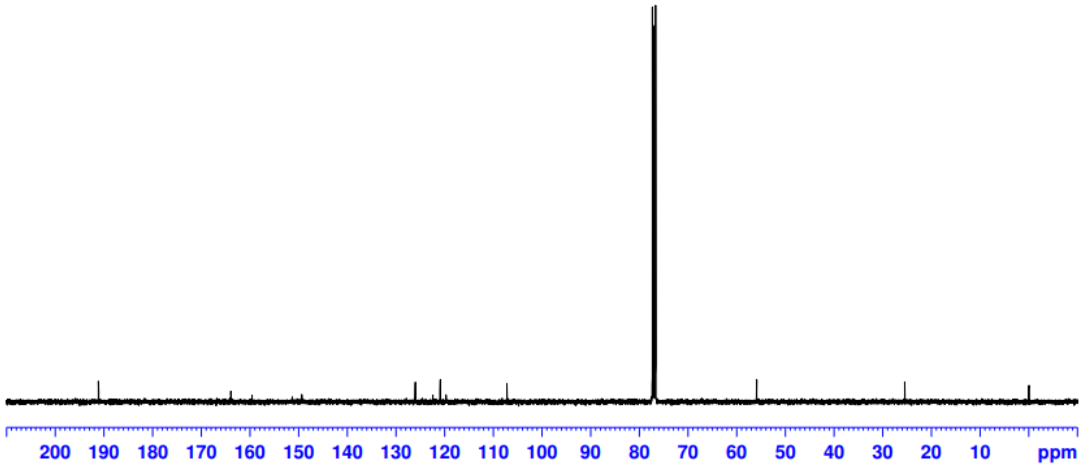

Figure 23. [13]C NMR of Aldehyde. [13]C NMR (CDCl3, 400 MHz) *δ* 25.495 (s), 55.926 (s), 77.020 (t), 107.243 (s), 119.740 (s), 120.942 (s), 122.465 (s), 126.064 (s), 149.311 (s), 159.551 (s), 163.876 (s), 191.084 (s).

TBSMAC to Create Side Chain at C3 on the Aldehyde

The reaction yielded 410.4 mg of ethyl-2-((tert-butyldimethylsilyl)oxy)-2-(4-chloro-7-methoxy-2-methylquinolin-3-yl)acetate (6). The solvent's distance from the baseline was 4.2 cm, and the product's distance was 2.8 cm, which was seen in the UV light and after CAM staining. The percent yield was 100.0%. **Figure 25** and **Figure 26** below shows the [1]H NMR and [13]C NMR of the compound.

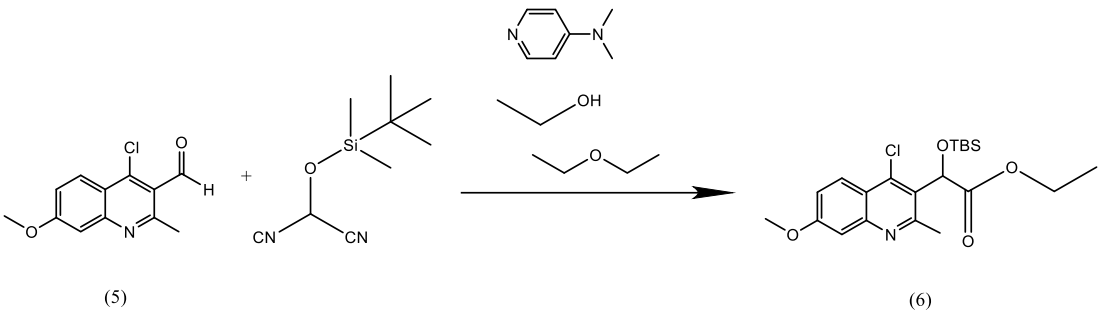

(5) (6)

Figure 24. Scheme of TBSMAC Addition Reaction.

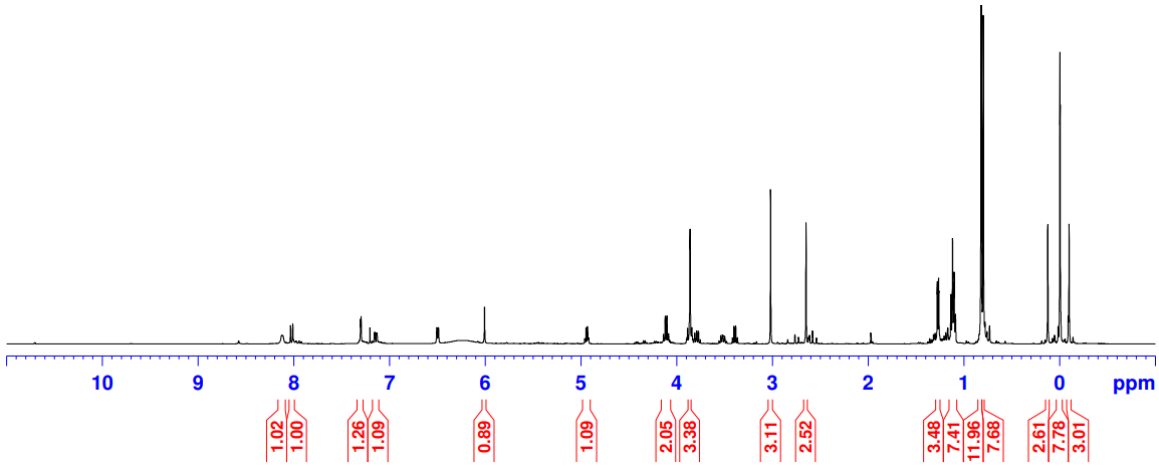

Figure 25. [1]H NMR of TBSMAC Addition. [1]H NMR (CDCl3, 400 MHz) δ 3.022 (s, 3H, CH3), 3.863 (s, 3H, OCH3), 4.187 (q, J = 0.8 Hz, 2H, OCH2CH3), 6.010 (s, 1H, OTBSCHO), 7.156 (dd, J = 2.4, 9.2 Hz, 1 H, arCH), 7.338 (d, J = 2.4 Hz, 1 H, arCH), 8.022 (d, J = 9.2 Hz, 1 H, arCH).

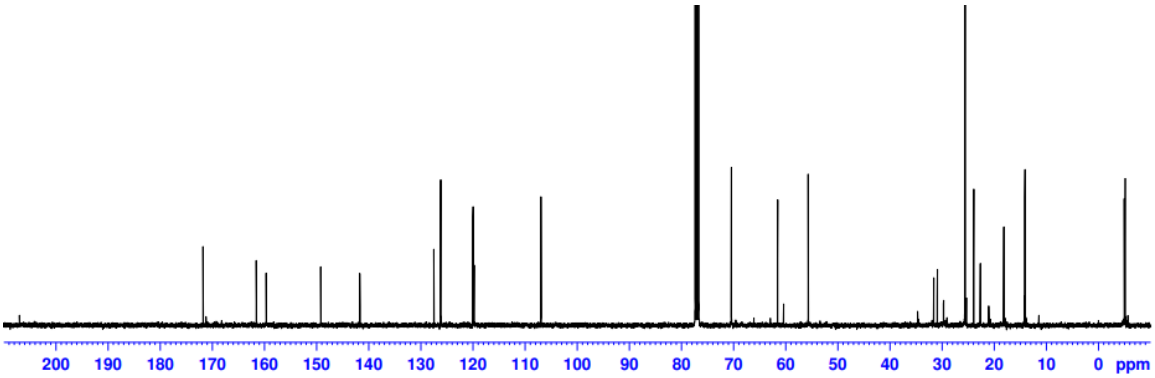

Figure 26. [13]C NMR of TBSMAC Addition. [13]C NMR (CDCl3, 400 MHz) *δ* 14.101 (s), 18.137 (s), 21.039 (d), 22.651 (s), 23.926 (s), 25.581 (s), 29.702 (s), 30.912 (s), 31.585 (s), 34. 665 (d), 55.670 (s),

60.388 (s), 61.552 (s), 70.411 (s), 106.869 (s), 119.917 (d), 126.111 (s), 127.430 (s), 141.623 (s), 149.136 (s), 159.600 (s), 161.481 (s), 171.705 (s).

Hydroxylation of the TBS Protecting Group on Ethyl Ester Side Chain

The reaction yielded 29.2 mg of ethyl 2-(4-chloro-7-methoxy-2-methylquinolin-3-yl)-2-hydroxyacetate (7). The percent yield was 9.73% here. Fractions 5-7 and 13-17 contained the desired product that was seen from the TLC. **Figure 28** and **Figure 29** below shows the ^{1}H NMR and ^{13}C NMR of the compound.

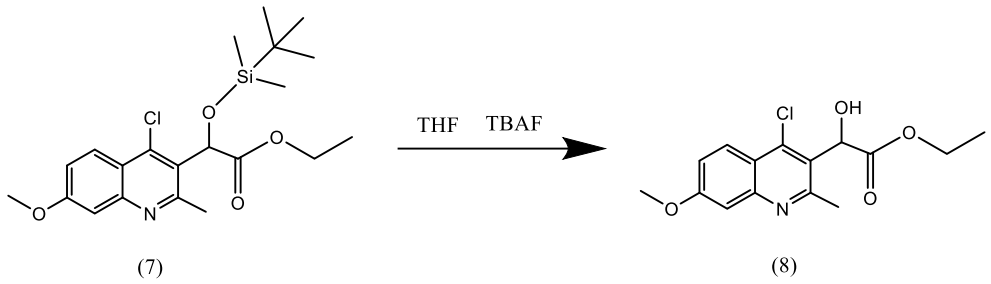

(7) (8)

Figure 27. Scheme of Hydroxylation of Quinoline Reaction.

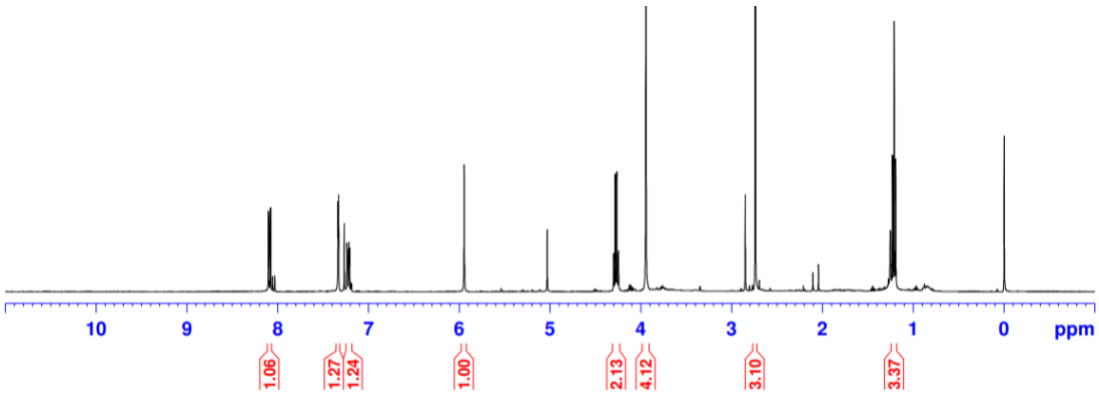

Figure 28. ^{1}H NMR of Hydroxylation on Quinoline. ^{1}H NMR (CDCl3, 400 MHz) δ 1.213 (t, J = 6.8 Hz, 3H, CH2CH3), 2.741 (s, 3H, CH3), 3.946 (s, 3H, OCH3), 4.275 (dd, J = 7.2, 14.4 Hz, 2H, OCH2CH3), 5.947 (s, 1H, CHOH), 7.225 (dd, J = 12, 14.4 Hz, 1 H, arCH), 7.334 (d, J = 2.4 Hz, 1 H, arCH), 8.100 (d, J = 9.2 Hz, 1 H, arCH).

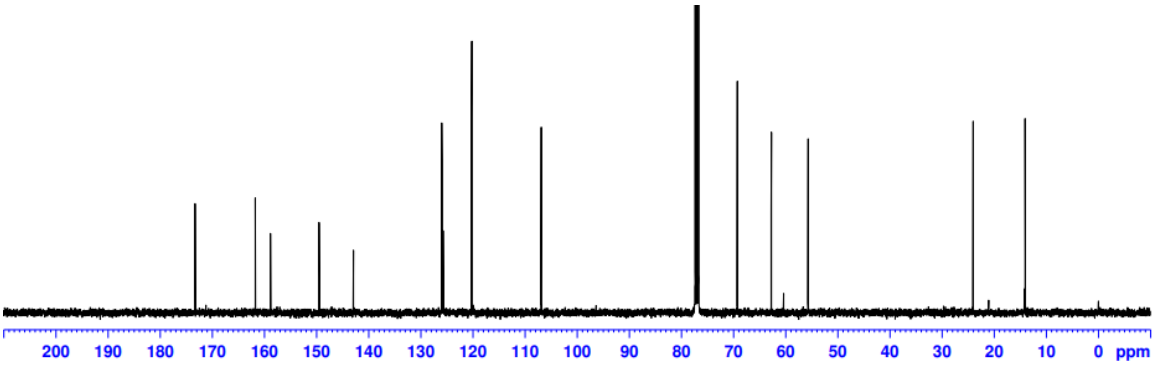

Figure 29. ^{13}C NMR of Hydroxylation of TBS Group. ^{13}C NMR (CDCl3, 400 MHz) δ 14.047 (s), 24.037 (s), 55.688 (s), 62.755 (s), 69.274 (s), 106.833 (s), 120.170 (s), 125.883 (s), 142.866 (s), 149.427 (s), 158.783 (s), 161.696 (s), 173.251 (s).

Chiral Coupling of the Quinoline at the CH position

147.8 mg of compound composed of ethyl (S)-2-4-(4-chloro-7-methylquinolin-3-yl)-2-(((((1R,2S,5R)-2-isopropyl-5-methylcyclohexyl)oxy)carbonyl)oxy)acetate (8) and ethyl (R)-2-4-(4-chloro-7-methylquinolin-3-yl)-2-(((((1R,2S,5R)-2-isopropyl-5-methylcyclohexyl)oxy)carbonyl)oxy)acetate (9) was measured after drying. This meant a percent yield of 110%.

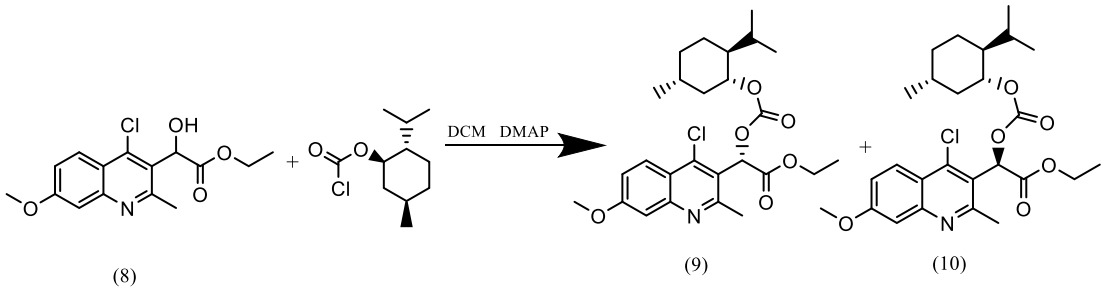

(8) (9) (10)

Figure 30. Scheme of Chiral Coupling Reaction.

CHAPTER V: DISCUSSION

Preparation of Isatoic Anhydride

Starting from the commercially available 2-amino-4-methoxybenzoic acid with bis(trichloromethyl) carbonate the isatoic anhydride, 7-methoxy-2H-benzo[d][1,3]oxazine-2,4(1H)-dione (1), was successfully created. The presence of the singlet at 12 ppm indicating the amino group, the three benzylic signals from 6.5 ppm- 8 ppm, and the methyl group singlet at 3.8 ppm showed characteristic peaks of the target isatoic anhydride. The disappearance of the hydroxyl group hydrogen peak that was present on the starting 2-amino-4-methoxybenzoic acid further indicated that the target molecule was formed. The product gave some sort of inorganic impurity that was not visible on the ^{1}H NMR, which gave a 110% yield with 15.5 g. The reaction gave pure components of 7-methoxy-2H-benzo[d][1,3]oxazine-2,4(1H)-dione (2) sufficient to precede with quinoline formation.

Preparation of quinoline

Starting from the isatoic anhydride 7-methoxy-2H-benzo[d][1,3]oxazine-2,4(1H)-dione (2) made in the first reaction and DMF with NaOH, ethyl 4-hydroxy-7-methoxy-2-methylquinoline-3-carboxylate was created. After taking the ^{1}H NMR, the amino proton peak previously seen at 12 ppm had disappeared while the singlet methyl group coming off the nitrogen ring showed a signal at 8 ppm. The presence of both the ethyl and methyl group at 4.2 ppm and 1.3 ppm further signified the intended quinoline was formed in 53% yield and of sufficient purity to continue with the chlorination reaction.

Chlorination of Quinoline

Beginning with ethyl 4-hydroxy-7-methoxy-2-methylquinoline-3-carboxylate (2), ethyl 4-chloro-7-methoxy-2-methylquinoline-3-carboxylate (3) was created using phosphoryl chloride. The product gave some sort of inorganic impurity that was not visible on the ^{1}H NMR, which gave a 112.2% yield with 13.25 g. The ^{1}H NMR showed a downfield shift in previously present compound due to the chloride group replacing the alcohol group. Impurities did not show on the ^{1}H NMR, which may signal that they are inorganic. The peaks gave proof that the desired compound had been formed.

Reduction of Ethyl Ester on Quinoline to Benzyl Alcohol

Starting with the ethyl 4-chloro-7-methoxy-2-methylquinolin-3-carboxylate (3), the target compound, (4-chloro-7-methoxy-2-methylquinolin-3-yl) methanol (4) was identified. The percent yield was 26.7%, which may be due to incomplete reaction, product loss, or impurities. The presence of the CH_2 group at 5 ppm and the disappearance of the ester ethyl and methyl protons at around 1 and 4 ppm signaled the target compound was made. The benzyl alcohol did not appear on the ^{1}H NMR, which was seen repeated times through previous completions of this step. Impurities were also heavily seen on the ^{1}H NMR.

Primary Alcohol Oxidation to Aldehyde

Starting with (4-chloro-7-methoxy-2-methylquinolin-3-yl) methanol (4), the target compound, 4-chloro-7-methoxy-2-methylquinoline-3-carbaldehyde (5) was identified. Once again, the percent yield was relatively high at 75%, where small traces of magnesium sulfate may still have been present. However, on the ^{1}H NMR,

the presence of a sharp peak at 10.7 ppm of an aldehyde proton and the disappearance of the ethyl protons signaled that the target compound formed.

TBSMAC to Create Side Chain at C3 on the Aldehyde

Beginning with 4-chloro-7-methoxy-2-methylquinoline-3-carbaldehyde (5), the target compound, ethyl-2-((tert-butyldimethylsilyl)oxy)-2-(4-chloro-7-methoxy-2-methylquinolin-3-yl)acetate (6), was created. After taking a TLC, the Rf value was observed to be 0.67. On the ^{1}H NMR, the CH proton peak at 6 ppm proved the consumption of the aldehyde and the addition of OTBS group on the benzylic position, and the quartet around 4.1 ppm signally the 2 protons of the ethyl group and the methyl group protons signaled at 1.2 ppm show the existence of the ethyl ester side chain.

Hydroxylation of the TBS Protecting Group on Ethyl Ester Side Chain

Beginning with ethyl-2-((tert-butyldimethylsilyl)oxy)-2-(4-chloro-7-methoxy-2-methylquinolin-3-yl)acetate (6), the target compound, ethyl 2-(4-chloro-7-methoxy-2-methylquinolin-3-yl)-2-hydroxyacetate (7), was created. On the ^{1}H NMR, characteristic peaks of the CH group around 6 ppm, and the quartet around 4.2 signally the 2 protons of the ethyl group and the methyl group protons signaled at 1.2 ppm show the existence of the ethyl ester side chain. Additionally, this successful reaction was observed to completion as the Rf value of the TLC was 0.23, signaling that the product did not move as far up the baseline (only 0.9 cm compared to 2.8 cm of the starting material) as the starting material observed in the TBSMAC addition, which had a Rf of 0.67. This smaller Rf of 0.23 signified that the product was more polar than the starting material, which is characteristic of the addition of the alcohol

group. CAM staining allowed for the product's movement of the baseline to be better seen to not move far from the baseline.

Chiral Coupling of the Quinoline at the CH position

After a TLC was ran of the progress of the reaction, two distinct dots seemed to form under the UV light, which hinted at the potential presence of the two diastereomers, and a ^{1}H NMR was ran. However, upon observance of the ^{1}H NMR, the peaks around 6 ppm did not drastically shift compared to the starting material NMR of the hydroxylation of the TBS group, which signaled that the two diastereomers did not separate as planned. This is indicated by the blue arrow below. There were also impurities in the compound signaled by the 110% yield. Additional TLC and reaction work up need to be done to continue this process of separation. This was unable to be continued due to time restraints.

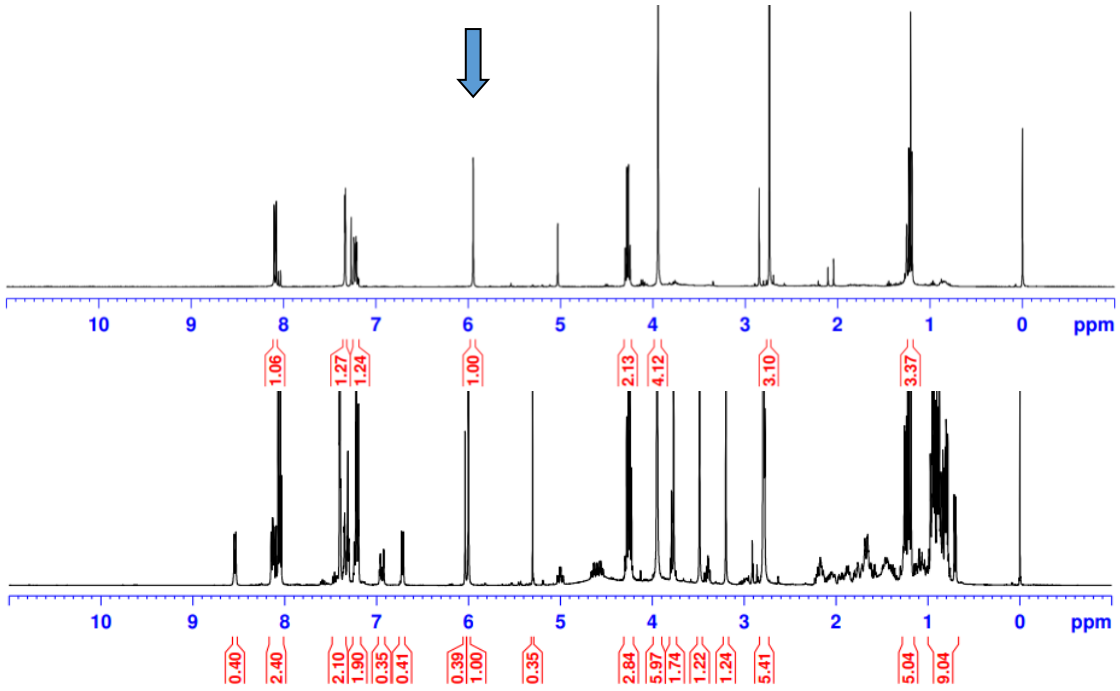

Figure 31. Comparison of ^{1}H NMRs from the Hydroxylation Starting Material and Chiral Coupling.

CHAPTER VI: FUTURE WORK

Within this thesis work, the diastereomers have been created and attempted to be separated. However, the attempts at separating them have been unsuccessful, and the compounds remain to be separated. Upon separation by either furthering the chiral coupling reaction or using an HPLC, the diastereomers should separate and show distinct shifted peaks on the NMR. With the R and S diastereomers separated, they would need to be identified on which is R vs. S by comparing the ^{13}C NMR of the compound to the Mosher ester model to determine absolute stereochemistry.

Each would then be separately assayed with Jacques Kessl's protocol who is a collaborator with the Donahue Research Group on the HIV-1 project, to determine what the multimerization effects are on IN. Then, back calculating will need to be conducted on how both R and S affect the racemic multimerization data. S is hypothesized to be more active, so it will need to be determined on how is the R diastereomer is affecting/depleting that. Both should then be taken on separately to form a fully functioning quinoline. The more active diastereomer, in this case it is thought to be the S, can then be used in further creation of HIV-1 drugs determined at affected the LEDGF/p75 binding pocket of IN by inducing multimerization.

REFERENCES

[1] Global HIV epidemic. Accessed 1 October 2022. https://www.who.int/data/gho/data /themes/hiv-aids.

[2] Frank, K. HIV life cycle: overview. *Encyclopedia of AIDS*. **2013.**

[3] Arts, E. J.; Hazuda, D. J. HIV-1 antiretroviral drug therapy. *Cold Spring Harb Perspect Med*. **2012**, 2, 1-23.

[4] Guidelines for the use of antiretroviral agents in adults and adolescents with HIV. Accessed 18 September 2022. https://clinicalinfo.hiv.gov/en/guidelines/hiv-clinical-guidelines-adult-and-adolescent-arv/what-start-initial-combination-regimens?view=full.

[5] McColl, D. J.; Chen, X. Strand transfer inhibitors of HIV-1 integrase: Bringing IN a new era of antiretroviral therapy. *Antivir. Res.* **2010**, 85, 101-118.

[6] Sun, J.; Patel, K.; Hume, J.; Pigza, J. A.; Donahue, M. G.; Kessl, J. J. Optimized binding of substituted quinoline ALLINIs within the HIV-1 integrase oligomer. *J. Biol. Chem.* **2021**, 296, 1-11.

[7] Engelman, A. N.; Kessel, J. J.; Kvaratskhelia, M. Allosteric inhibition of HIV-1 integrase activity. *Curr. Opin. Chem. Biol.* **2014**, 17, 339-345.

[8] Englelman, A. N. Multifaceted HIV integrase functionalities and therapeutic strategies for their inhibition. *J. Biol. Chem.* **2019**, 294, 151137-15157.

[9] Serrao, E.; Odde, S.; Ramkumar, K.; Neamati, N. Raltegravir, elvitegravir, and metoogravir: the birth of" me-too" HIV-1 integrase inhibitors. *Retrovir*. **2009,** *6*, 1-14.

[10] Lennox, J.L.; DeJesus, E.; Lazzarin, A.; Pollard, R.B.; Madruga, J.V.R.; Berger, D.S.; Zhao, J.; Xu, X.; Williams-Diaz, A.; Rodgers, A.J.; Barnard, R.J. Safety and efficacy of raltegravir-based versus efavirenz-based combination therapy in treatment-naive patients with HIV-1 infection: a multicentre, double-blind randomised controlled trial. *The Lancet*. **2009**, 374, 796-806.

[11] Zolopa, A.; Sax, P.; DeJesus, E.; Mills, A.; Cohen, C.; Wohl, D.; Gallant, J.E.; Liu, H. C.; Plummer, A.; White, K. L.; Cheng, A. K. A randomized double-blind comparison of coformulated elvitegravir/cobicistat/emtricitabine/tenofovir disoproxil fumarate versus efavirenz/emtricitabine/tenofovir disoproxil fumarate for initial treatment of HIV-1 infection: analysis of week 96 results. *JAIDS.* **2013**, 63, 96-100.

[12] Walmsley, S.L., Antela, A., Clumeck, N., Duiculescu, D., Eberhard, A., Gutiérrez, F., Hocqueloux, L.; Maggiolo, F.; Sandkovsky, U.; Granier, C.; Pappa, K. Dolutegravir plus

abacavir–lamivudine for the treatment of HIV-1 infection. *N. Engl. J. Med.* **2013**, 369, 1807-1818.

[13] Cahn, P.; Pozniak, A.L.; Mingrone, H.; Shuldyakov, A.; Brites, C.; Andrade-Villanueva, J.F.; Richmond, G.; Buendia, C.B.; Fourie, J.; Ramgopal, M.; Hagins, D. Dolutegravir versus raltegravir in antiretroviral-experienced, integrase-inhibitor-naive adults with HIV: week 48 results from the randomised, double-blind, non-inferiority SAILING study. *The Lancet*. **2013**, 382, 700-708.

[14] Cabenuva (cabotegravir and rilpivirine) for the treatment of HIV-1 infection, USA. Accessed 5 February 2023. https://www.clinicaltrialsarena.com/projects/cabenuva-cabotegravir-rilpivirine/.

[15] Koneru, P. C.; Francis, A. C.; Deng, N.; Rebensburg, S. V.; Hoyte, A. C.; Lindenberger, J.; Adu-Ampratwum, D., Larue, R. C.; Wempe, M. F.; Engelman, A. N.; Lyumkis, D.; Fuchs, J. R.; Levy, R. M.; Melikyan, G. B.; Kvaratskhelia, M. HIV-1 integrase tetramers are the antiviral target of pyridine-based allosteric integrase inhibitors. *eLife.* **2019,** 8, 1-27.